EPJ Web of Conferences **60**, 19005 (2013)
DOI: 10.1051/epjconf/20136019005

Measurement of Inclusive W and Z Production in ATLAS

J. R. Goddard[1,a] on behalf of the ATLAS Collaboration

[1] *Queen Mary, University of London, Mile End Road, London. E1 4NS.*

Abstract. A summary of five ATLAS W and Z inclusive measurements are presented, these are a mixture of analyses using the 2010 and 2011 datasets of $\sqrt{s}$ = 7 TeV proton-proton collisions at the LHC. The 2010 data is used to measure the cross sections of the Z, W^+ and W^- bosons which are then used with the HERA deep inelastic scattering data to determine the strange quark density of the proton. Three analyses that use 2011 data are shown; a measurement of the forward-backward asymmetry of the Z/γ^* boson, from which the effective weak mixing angle is extracted; a measurement of the angular correlations of Drell-Yan lepton pairs from resonant Z decays; and a measurement of the high mass Drell-Yan differential cross section.

1 Introduction

Measurements of electroweak processes, such as those summarised here from ATLAS [1] are important for probing the standard model in the new energy regime of the LHC and improve the theoretical predictions with additional constraints. Furthermore the proton Parton Distribution Functions (PDFs) which are extrapolated from the phase space of previous experiments can be constrained by measurements such as these, as clearly seen in sections 2 and 3.

2 Inclusive W and Z Cross Section Measurements

The Z, W^+ and W^- production cross sections have been measured both inclusively and differentially in the electron and the muon decay channels [2] using about 35 pb^{-1} of 2010 data. The separate channels are corrected to a common region in phase space and then combined using a χ^2 minimisation method. The common phase space region is defined as $p_T^l > 20$ GeV and $66 < m_{ll} < 116$ GeV for the Z bosons, where p_T^l is the transverse momentum of the leptons and m_{ll} is the invariant mass of the lepton pair. The $W^\pm$ decays are required to have $p_T^l > 20$ GeV, $p_T^\nu > 25$ GeV and $m_T^{l\nu} > 40$ GeV, where p_T^l (p_T^ν) and $m_T^{l\nu}$ are the transverse momentum of the charged lepton (neutrino) and the transverse mass of the lepton-neutrino pair. Fig. 1 shows the fiducial inclusive cross sections of the Z and $(W^+ + W^-)$ plotted against each other. The uncertainty is dominated by the $\sim 1\%$ systematic uncertainty (excluding the 3.4% luminosity uncertainty). The measurement is compared to theoretical predictions obtained from next-to-next-to-leading-order (NNLO) `FEWZ2.0` [3] with either the MSTW2008 [4], HERAPDF1.5 [5], ABKM09 [6] or JR09 [7] NNLO PDF sets. It is evident from the plot that the measurement has the power to distinguish between the different PDFs. The differential cross sections have been

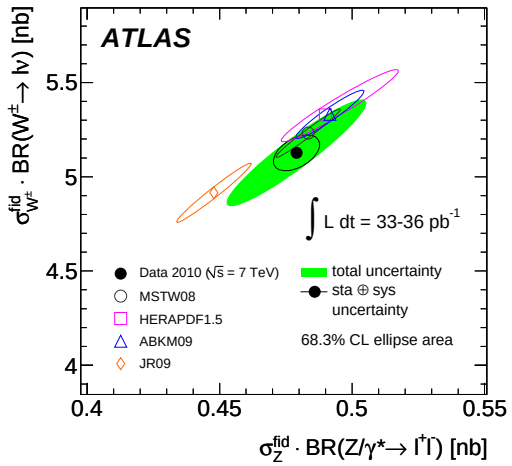

Figure 1. Combined electron and muon fiducial inclusive cross sections of the Z and the $W^+ + W^-$ bosons. The total uncertainty includes the luminosity systematic uncertainty [2].

measured as a function of the pseudorapidity, η, of the charged lepton for the $W^\pm$ decays and as a functon of the rapidity, y, of the Z boson for the Z decays. These can be seen for the combined electron and muon channels $W^\pm$ decays in fig. 2 compared with calculated predictions, which use a combination of NNLO `FEWZ` and `DYNNLO` [8, 9]. The typical data precision is about 2%. The uncertainties shown for the theoretical predictions are a convolution of the PDF uncertainties, considered by the authors of the various PDF sets to correspond to 68% CL, and a residual numerical uncertainty of below 0.5%. There is broad agreement between the data and the theoretical predictions

[a] e-mail: j.goddard@qmul.ac.uk

but again data demonstrate the ability to discriminate between different PDF sets. The importance of measuring the cross sections of the W^+ and W^- bosons separately can be seen, as the level of agreement with the theoretical predictions differs between the two.

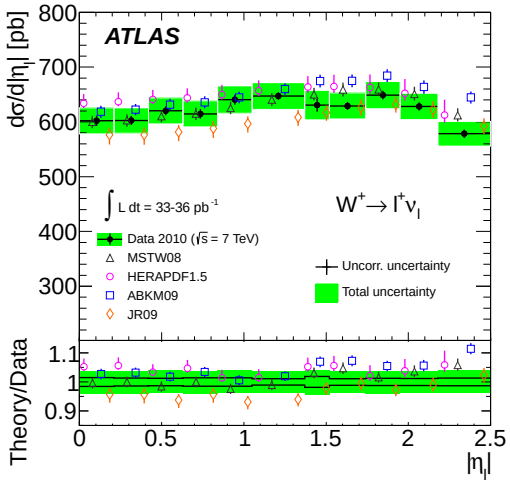

(a) $W^+ \to l^+\nu_l$

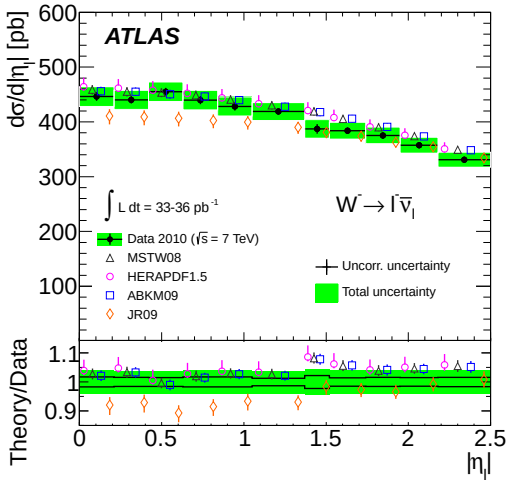

(b) $W^- \to l^-\bar{\nu}_l$

Figure 2. Combined electron and muon fiducial differential cross sections of the $W^+ \to l^+\nu_l$ and $W^- \to l^-\bar{\nu}_l$ processes [2].

3 Determination of the Strange Quark Density of the Proton

If one assumes SU(3) flavour symmetry, the light quark sea distributions in the proton should be equal, but due to their higher mass, the strange quarks may be suppressed. Information for this currently comes from neutrino scattering experiments which probe the proton in a higher x region than the analysis described here [10]. The Z, W^+ and W^- cross section measurements described in the previous section are used with the deep inelastic scattering data from the H1 and ZEUS experiments at HERA [5]. Two NNLO PDF fits are performed using the `HERAFitter` framework [5, 11]. The first fit, referred to as the *fixed* $\bar{s}$ *fit*, fully couples the strange quark sea with the down quark sea by setting $\bar{s}/\bar{d} = 0.5$, where $\bar{s}$ and $\bar{d}$ are the anti-strange and anti-down sea quark distributions respectively. The second fit, referred to as the *free* $\bar{s}$ *fit*, parameterises $x\bar{s}$ with two free strangeness parameters. Both fits assume $xs = x\bar{s}$ by default and both have good χ^2 per degree of freedom giving 546.1/567 with 13 free parameters for the fixed $\bar{s}$ fit and 538.4/565 with 15 degrees of freedom for the free $\bar{s}$ fit. However, when considering the partial χ^2 from only the ATLAS data, it is seen that the data prefers the free $\bar{s}$ fit, giving $\chi^2 = 44.5$ for 30 data points for the fixed $\bar{s}$ fit which significantly improves to 33.9 for the free $\bar{s}$ fit. Fig. 3 shows the Z differential cross section from section 2 compared to predictions from the two fits. It can be seen that the free $\bar{s}$ fit does a better job in describing the data. The level of suppression of the strange sea can

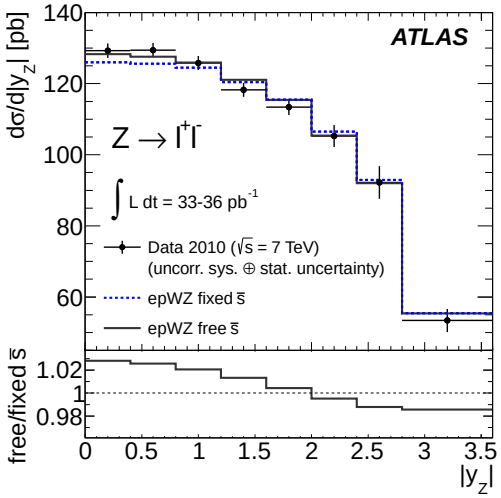

Figure 3. Combined fiducial differential cross section of $Z \to l^+l^-$ decays compared to predictions from the two NNLO PDF fits [10].

be determined from the free $\bar{s}$ fit by considering the ratio $r_s = 0.5(s+\bar{s})/\bar{d}$, which is found to be $r_s = 1.00^{+0.25}_{-0.28}$, when evaluated at the intial scale of 1.9 GeV and $x = 0.023$. The uncertainty on r_s is dominated by an experimental uncertainty of ±0.20. This is consistent with no suppression of the strange quark sea at very low x. This value of r_s is compared to those obtained from other PDF sets in fig. 4, where it can be seen that only CT10 [12] is in agreement, while ABKM09, NNPDF2.1 [13, 14] and MSTW2008 all have much smaller values of r_s. These differences arise from the variation in the treatment of the strange quark sea suppression in the different fits.

4 Forward-Backward Asymmetry of Z/γ^* Decays

Due to the V-A nature of the weak interaction, the Z couples differently to left and right handed fermions, resulting in a forward backward asymmetry of the $q\bar{q} \to Z/\gamma^* \to l^+l^-$ process with respect to the direction of the incoming quark. The asymmetry, A_{FB}, is expressed as $A_{FB} = \frac{\sigma_F - \sigma_B}{\sigma_F + \sigma_B}$,

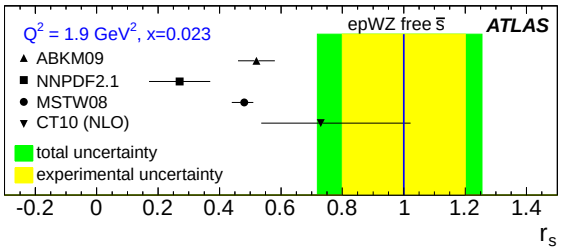

Figure 4. Comparison of the value of r_s obtained from a number of different PDF sets [10].

where σ_F and σ_B are the cross sections in the forward and backward directions respectively. The analysis presented here [15] used 4.8 fb^{-1} of data recorded in 2011. The analysis measures the forward-backward asymmetry in three different channels. The *CC Electron Channel* considers two electrons in the centre of the detector, requiring kinematic cuts on both electrons of $E_T > 25$ GeV and $|\eta| < 2.47$ excluding $1.37 < |\eta| < 1.52$, where E_T is the transverse energy. The *CF Electron Channel* requires one electron to be in the centre of the detector (passing the CC requirements) and one in the forward region, requiring $E_T > 25$ GeV and $2.5 < |\eta| < 4.9$ excluding $3.16 < |\eta| < 3.35$. Finally, the *Muon Channel* requires both muons to be in the centre of the detector, giving a kinematic region of $p_T > 20$ GeV and $|\eta| < 2.4$. The forward-backward asymmetry is calculated for each channel, this is then unfolded to the Born level, as shown in fig. 5. The data is compared to `Pythia6.4` [16] MC with NNLO k-factors applied which are calculated with `PHOZPR` [17] using MSTW2008 PDFs. It is clear from the ratio Δ/σ in the lower section of the plots in fig. 5 that there is good data and MC agreement, where Δ is the difference between data and MC and σ is the quadratic sum of the data and MC uncertainties. The measurement of the forward-backward asymmetry allows the effective electroweak mixing angle to be extracted. This is the electroweak mixing angle, commonly defined as $\sin^2\theta_W = 1 - \frac{m_W^2}{m_Z^2}$, with higher order loop corrections included. To extract the electroweak mixing angle the A_{FB} dependence on m_{ll} is used before the unfolding to the Born level. It is compared to a number of MC templates using a χ^2 test in an invariant mass range of $70 < m_{ll} < 250$ GeV, with each template produced with a different value of $\sin^2\theta_W^{eff}$. Each of the three channels are fitted and then combined to give a single value of $\sin^2\theta_W^{eff}$, these are compared to previous results in fig. 6. The three channels show good agreement and the combined result has a value of $\sin^2\theta_W^{eff} = 0.2297 \pm 0.0010$ which has a 0.17% statistical uncertainty and a 0.39% systematic uncertainty, dominated by the PDF uncertainty. The combined measurement is in good agreement with the CMS and DØ results and only 1.8σ from the PDG global fit value [18]. This is currently the most precise measurement of $\sin^2\theta_W^{eff}$ from a LHC experiment and the first hadron collider measurement to combine the electron and muon channels when measuring $\sin^2\theta_W^{eff}$ at the Z resonance.

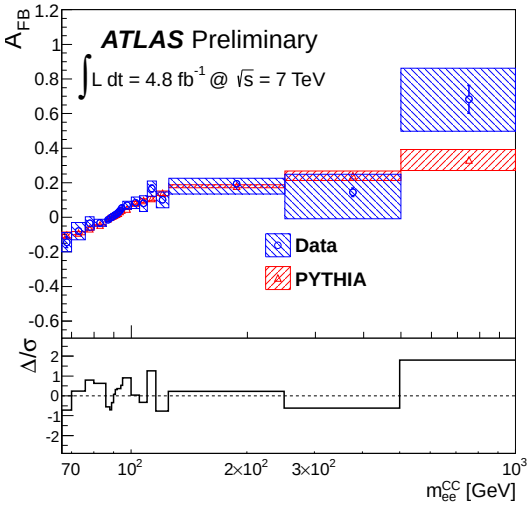

(a) CC Electron Channel

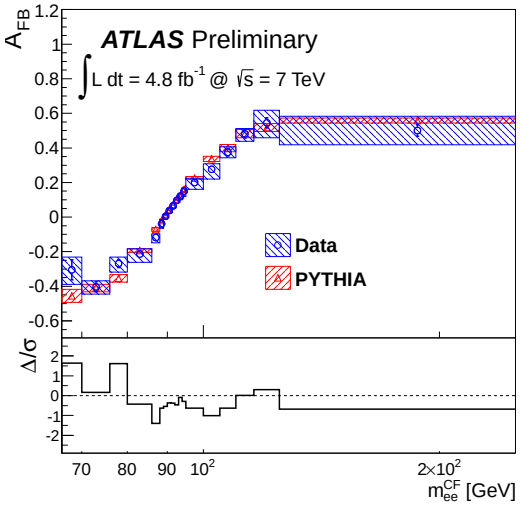

(b) CF Electron Channel

Figure 5. Forward-backward asymmetry distributions unfolded to the Born level for the CC and CF electron channels [15].

5 Angular Correlation of Drell-Yan Lepton Pairs

Previous measurements of the p_T of the W and Z vector bosons [19, 20] have demonstrated the difficulty theoretical predictions have in describing those distributions; understanding of which is important for W mass measurements. In the analysis presented here [21] the ϕ_η^* variable, previously used at the DØ experiment is examined. The variable is defined as $\phi_\eta^* \equiv \tan(\phi_{\text{acop}}/2) \cdot \sin(\theta_\eta^*)$, where $\phi_{\text{acop}} \equiv \pi - \Delta\phi$ and $\cos(\theta_\eta^*) \equiv \tanh[(\eta^- - \eta^+)/2]$, with $\Delta\phi$ being the difference in the azimuthal angle between the leptons, and $\eta^\pm$ being the pseudorapidity of each lepton.

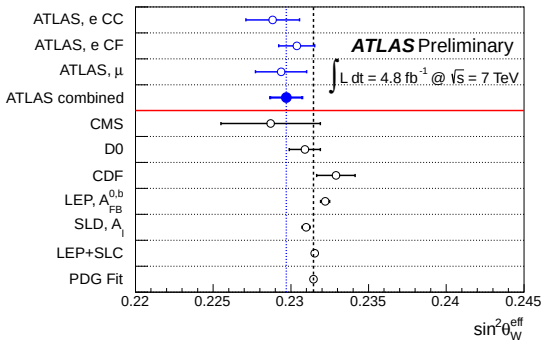

Figure 6. Values of $\sin^2\theta_W^{eff}$ obtained in the different channels and combined. Comparison to values obtained by other experiments is also shown [15].

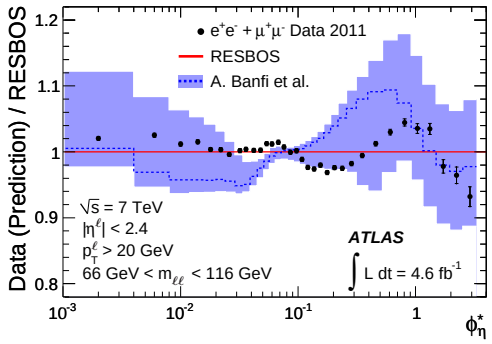

Figure 7. Ratio of $1/\sigma^{fid} \cdot d\sigma^{fid}/d\phi_\eta^*$ from data and an analytical QCD calculation to RESBOS [21].

As such, ϕ_η^* is dependant only on the angles of the two leptons which can be measured with much better resolution than the momentum, particularly at low p_T. The ϕ_η^* variable is correlated with p_T^Z/m_{ll}, allowing the same physics to be probed. The differential cross section is measured as a function of ϕ_η^* in the electron and muon channels. A kinematic region of $p_T^l > 20$ GeV and $|\eta^l| < 2.4$ is used at the Z resonance in the invariant mass range $66 < m_{ll} < 116$ GeV using 4.6 fb^{-1} of 2011 data. The normalised differential cross section, $1/\sigma^{fid} \cdot d\sigma^{fid}/d\phi_\eta^*$, was determined from data and from an analytical QCD prediction [22], these are compared to the prediction from RESBOS [23], as shown by the ratio in fig. 7. RESBOS resums the next-to-next-to-leading-logarithms (NNLL) and matches to a leading order QCD result, with k-factors correcting to next-to-leading order (NLO), while the analytical prediction contains NNLL matched to an NLO QCD result from MCFM [24]. The experimental uncertainty is statistically dominated, with a statistical uncertainty between 0.30% and 1.61%; the systematic uncertainty varies between 0.13% and 0.58%. The difference between the RESBOS prediction and the data is smaller than the RESBOS PDF uncertainty, which varies from 4% to 6% for $\phi_\eta^* < 0.1$ and $\phi_\eta^* > 0.1$ respectively. The analytical calculation describes the data less well, but is still largely in agreement within the relatively large theoretical uncertainty. Neither prediction demonstrates the ability to describe the detailed shape of the distribution.

6 High Mass Drell-Yan Cross Section

The Drell-Yan differential mass cross section has been measured in the electron channel [25] in an invariant mass range of $116 < m_{ee} < 1500$ GeV with 4.9 fb^{-1} of 2011 data. A kinematic region of $|\eta_e| < 2.5$ and $p_T^e > 25$ GeV is used. This extends the standard model measurement of the Z resonance and is complementary to Z' searches. The measurement is sensitive to the behaviour of PDFs for $x \gtrsim 10^{-3}$ and higher order electroweak corrections. Fig. 8 shows the invariant mass distribution of the electron pair, where good agreement between data and MC can be seen. Pythia6.426 signal MC is used which is corrected with m_{ee} dependant NNLO k-factors including NLO electroweak corrections. Fig. 9 shows the differential mass

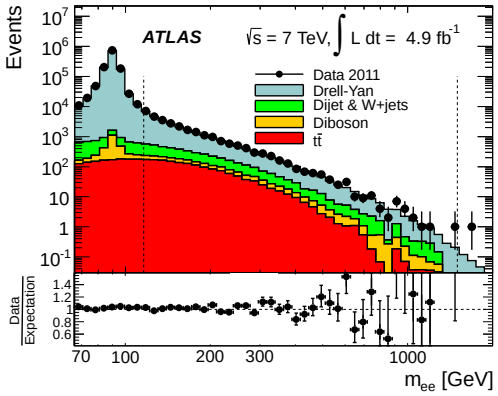

Figure 8. Invariant mass of the high mass Drell-Yan lepton pair [25].

cross section unfolded to the Born level. Comparisons to theoretical predictions are made using FEWZ3.1 [26] at NNLO using the G_μ electroweak scheme with a number of different PDF sets. The theoretical predictions have NLO electroweak corrections applied which take into consideration initial and final state QED radiation and interference between the two. Leading order photon induced corrections have also been applied using the MSTW2005qed PDF set [27]. The upper ratio plot shows the ratio of the theoretical predictions to the data, with predictions produced using either the MSTW2008, HERAPDF1.5, CT10, ABM11 [28] or NNPDF2.3 [29] PDF sets. It can be seen that the data is consistent with all of the PDF sets considered. The lower ratio plot demonstrates the importance of the photon induced corrections, with the dashed line showing the MSTW2008 prediction without the photon induced corrections. The corrections are of the order of the 68% CL uncertainty from the MSTW2008 error sets. ATLAS is the first LHC experiment to include these photon induced corrections to the theoretical predictions which this measurement demonstrates can be sizable.

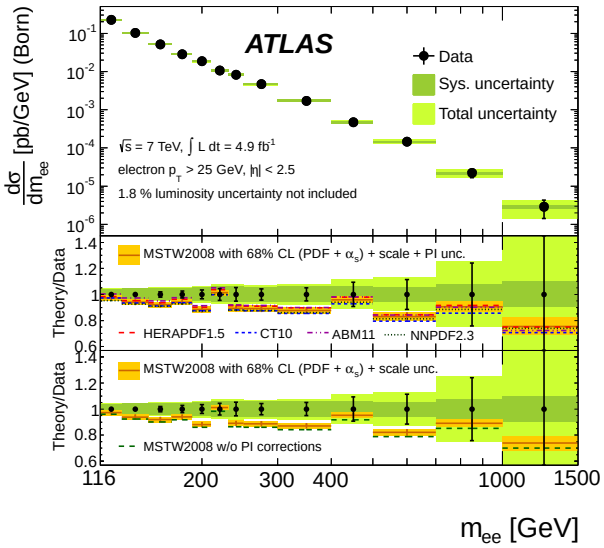

Figure 9. High mass Drell-Yan differential cross section as a function of mass with comparison to different PDFs. The importance of the photon induced corrections are also shown [25].

7 Conclusions

The analyses presented here cover a range of measurements of inclusive W and Z production at ATLAS. The inclusive cross section measurements show the potential to constrain the PDFs, this is then used to determine the strange quark density of the proton at small x which is found to be consistent with no suppression of the $\bar{s}$ PDF relative to $\bar{d}$. Measurement of the forward-backward asymmetry shows good consistency with the standard model predictions. A value of $\sin^2\theta_W^{eff}$ is extracted which is in agreement with other experiments and is currently the most precise measurement of $\sin^2\theta_W^{eff}$ from the LHC. The relative differential cross section, $1/\sigma^{fid}\cdot \mathrm{d}\sigma^{fid}/\mathrm{d}\phi_\eta^*$, is measured with small experimental uncertainties and while largely showing agreement with predictions demonstrates the current inability of theory to recreate the detailed shape of the ϕ_η^* differential cross section. Finally, the measurement of the high mass Drell-Yan differential cross section shows consistency with theoretical predictions using a number of PDF sets and demonstrates the importance of including photon induced corrections in theoretical predictions.

References

[1] ATLAS Collaboration, Journal of Instrumentation **3**, S08003 (2008)

[2] ATLAS Collaboration, Phys. Rev. **D85**, 072004 (2012), arXiv:1109.5141

[3] R. Gavin, Y. Li, F. Petriello, S. Quackenbush, Computer Physics Communications **182**, 2388 (2011)

[4] A.D. Martin, W.J. Stirling, R.S. Thorne, G. Watt, Eur. Phys. J. **C63**, 189 (2009), arXiv:0901.0002

[5] F.D. Aaron et al. (H1 and ZEUS Collaboration), JHEP **1001**, 109 (2010), arXiv:0911.0884

[6] S. Alekhin, J. Blumlein, S. Klein, S. Moch, Phys. Rev. **D81**, 014032 (2010), arXiv:0908.2766

[7] P. Jimenez-Delgado, E. Reya, Phys. Rev. D **79**, 074023 (2009)

[8] S. Catani, M. Grazzini, Phys. Rev. Lett. **98**, 222002 (2007), arXiv:hep-ph/0703012

[9] S. Catani, L. Cieri, G. Ferrera, D. de Florian, M. Grazzini, Phys. Rev. Lett. **103**, 082001 (2009), arXiv:0903.2120

[10] ATLAS Collaboration, Phys. Rev. Lett. **109**, 012001 (2012), arXiv:1203.4051

[11] F.D. Aaron et al. (H1 Collaboration), Eur. Phys. J. **C64**, 561 (2009), arXiv:0904.3513

[12] H.L. Lai et al., Phys. Rev. **D82**, 074024 (2010), arXiv:1007.2241

[13] R.D. Ball et al. (NNPDF Collaboration), Nucl. Phys. **B809**, 1 (2009), arXiv:0808.1231

[14] R.D. Ball et al. (NNPDF Collaboration), Nucl. Phys. **B855**, 153 (2012), arXiv:1107.2652

[15] ATLAS Collaboration, *ATLAS-CONF-2013-043* (2013), http://cds.cern.ch/record/1544035/

[16] T. Sjostrand, S. Mrenna, P.Z. Skands, JHEP **0605**, 026 (2006), arXiv:hep-ph/0603175

[17] R. Hamberg, W.L. van Neerven, T. Matsuura, Nucl. Phys. **B359**, 343 (1991)

[18] K. Nakamura et al, J. Phys. G **37**, 075021 (2010)

[19] ATLAS Collaboration, Phys. Lett. **B705**, 415 (2011), arXiv:1107.2381

[20] ATLAS Collaboration, Phys. Rev. **D85**, 012005 (2012), arXiv:1108.6308

[21] ATLAS Collaboration, Phys. Lett. **B720**, 32 (2013), arXiv:1211.6899

[22] A. Banfi, M. Dasgupta, S. Marzani, L. Tomlinson, Phys. Lett. **B715**, 152 (2012), arXiv:1205.4760

[23] F. Landry, R. Brock, G. Ladinsky, C.P. Yuan, Phys. Rev. **D63**, 013004 (2001), arXiv:hep-ph/9905391

[24] J.M. Campbell, R.K. Ellis, Phys. Rev. **D65**, 113007 (2002), arXiv:hep-ph/0202176

[25] ATLAS Collaboration (2013), arXiv:1305.4192

[26] C. Anastasiou, L.J. Dixon, K. Melnĩkov, F. Petriello, Phys. Rev. **D69**, 094008 (2004), arXiv:hep-ph/0312266

[27] A.D. Martin, R.G. Roberts, W.J. Stirling, R.S. Thorne, Eur. Phys. J. **C39**, 155 (2005), arXiv:hep-ph/0411040

[28] S. Alekhin, J. Blumlein, S. Moch, Phys. Rev. **D86**, 054009 (2012), arXiv:1202.2281

[29] R.D. Ball, V. Bertone, S. Carrazza, C.S. Deans, L. Del Debbio et al., Nucl. Phys. **B867**, 244 (2013), arXiv:1207.1303